

2014; Oleg Lupan,2008). Among the three crystalline forms of zinc oxide—hexagonal wurtzite, cubic zinc blende, and cubic rocksalt—the hexagonal wurtzite structure is the most thermodynamically stable, while the cubic rocksalt phase is rarely observed under ambient conditions (Ozqur U,2005). Literature survey elaborates about various fabrication methods that are employed for the deposition of ZnO thin films which includes sol-gel process (M.N. Kamalasanan,1996), spray pyrolysis (F.D. Paraguay,1999), chemical vapor deposition (CVD) (T. Minami,1994), molecular beam deposition (MBE) (K Nakamura,2000), and radio frequency (RF) magnetron sputtering (S. Maniv,1978; M.-S. Wu,1998). As the properties of thin films greatly rely on the fabrication conditions, radio frequency (RF) sputtering technique is a better method for growing ZnO thin films. Studies show that radio frequency sputtering technique have a good control over different fabricating parameters such as working pressure, deposition temperature, coating time, Ar: O₂ gas flow rate, and RF power (Shashikant Sharma,2014). The present work illustrates a study on structural and optical properties of post deposition annealing of ZnO thin films fabricated on glass substrates employing RF sputtering technique. Structural properties and optical parameters such as transmittance, optical bandgap, refractive index, extinction coefficient, optical conductivity of the as-prepared and annealed RF sputtered ZnO thin films have been examined and reported.

2 Experimental details

2.1 ZnO thin film preparation

ZnO thin films were fabricated on glass slides using RF sputtering technique. Substrates were thoroughly cleaned in a two-step ultrasonication process with organic solvents such as 2-propanol and acetone and was rinsed finally in deionized water before mounting it to the substrate holder placed in the vacuum chamber. ZnO ceramic target (2" dia,3mm thickness, 99.995% Kurt J Leskar company, Germany) equipped in a vacuum chamber with the help of diffusion pump to achieve a base pressure of 10⁻⁶mbar. Depositions were done by introducing mixed atmosphere of Argon and Oxygen in ratio was 20sccm:2sccm. Argon gas was used to create an inert atmosphere

while oxygen gas was introduced into the coating chamber in order to maintain the stoichiometry of the title compound. All the depositions were done by keeping the substrate -target distance fixed to 7cm under RF power of 80W for a coating time of 30minutes. Also, before every coating, target was pre-sputtered for 2minutes under 80W with an aim to remove the contaminants present on the target surface and to stabilize the system. Working pressure for each coating was 5×10^{-3} mbar. The depositions were done at room temperature and the ZnO thin films were subsequently annealed for 30 minutes in hot air oven at three different temperatures 100⁰C, 120⁰C, 140⁰C. Structural and optical properties of as prepared and annealed samples were systematically analyzed in order to explore the effect of heat treatment on the samples fabricated.

2.2 Thin film characterization

X-Ray Diffractometer (XRD Smart Lab, Rigaku) with a scanning range of 2θ set between 20° and 80° was used to characterize the crystal structure, Raman spectrophotometer (Horiba Labram HR Evo) was used to observe vibrational modes and thus giving the structural fingerprint of material under study. Optical characterization of ZnO thin films have been done using UV Visible spectrophotometer (SHIMADZU, JAPAN).

3 Results and discussion

3.1 Structural and surface morphology study

3.1.1 X-ray diffraction studies

Figure1(a) shows XRD spectra of as prepared and annealed RF sputtered ZnO thin films. The annealing temperatures chosen were 100°C, 120°C and 140°C. The spectra indicates that the fabricated ZnO thin films possess hexagonal wurtzite crystal structure. Annealing improved the intensity of the peaks, which indicates that the films have good quality and crystallinity. Comparison of XRD peaks and inter planar distance values of fabricated ZnO thin films and standard JCPDS data sheet (00-036-1451) is shown in table 1. From interplanar distances 'd'. lattice constants a and c, full width half-maximum (FWHM) values and crystallite size 'D'

were determined using Bragg equation and Debye Scherer formula (Cullity, B.D ,2001; Patterson, 1939).

$$2d\sin\theta=n\lambda \text{-----1}$$

The average grain size (D) values of the films were calculated from Debye- Scherrer's Formula

$$D = \frac{k}{\cos} \text{-----2}$$

Where k is the shape factor (0.9), $\Delta 2\theta$ is the full width half- maximum (FWHM), θ is the half of diffraction angle and λ is the wavelength of the X-ray. Table 2 shows the variation of crystallite size D with annealing temperature of ZnO thin films. The values suggest that with annealing process, the crystallite size D increased from 6.14 nm (as prepared ZnO thin film) to 7.57nm (annealed ZnO thin film at 140°C).

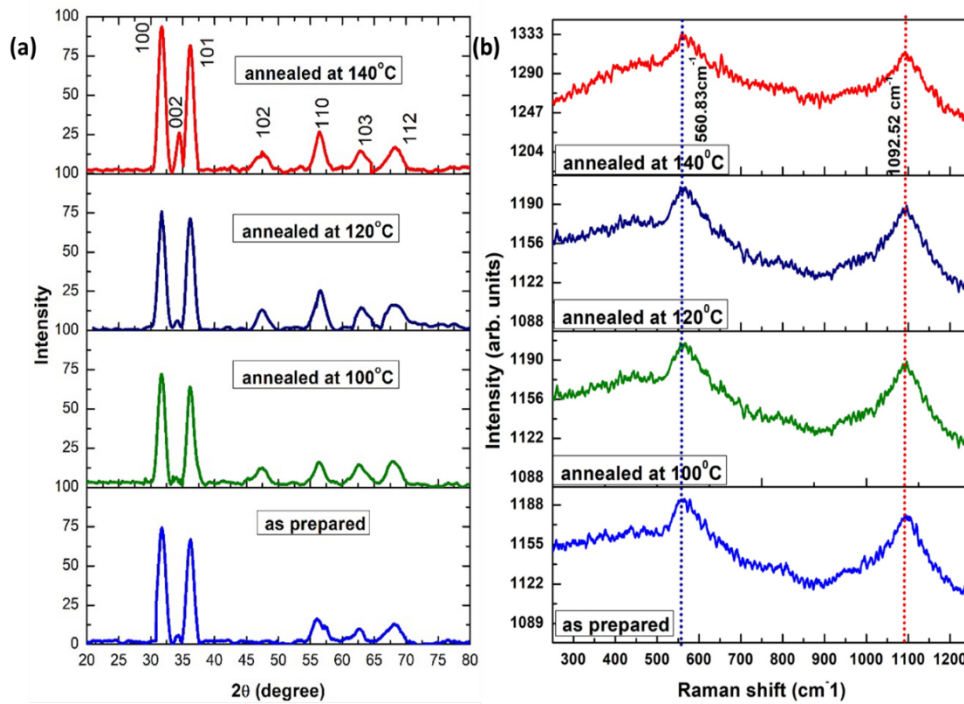


Figure1(a). XRD spectra of as prepared and annealed RF sputtered ZnO thin films
 Figure(b). Raman spectra of as prepared and annealed RF sputtered ZnO thin films

Sample	2theta(°)		d values (Å°)		Miller Planes
	Observed	Standard	Observed	Standard	
ZnO	31.85	31.82	2.81	2.81	(1 0 0)
	34.4	34.47	2.6	2.6	(0 0 2)
	36.34	36.19	2.47	2.48	(1 0 1)
	47.67	47.54	1.91	1.91	(1 0 2)
	56.62	56.4	1.62	1.63	(1 1 0)
	62.56	62.25	1.48	1.49	(1 0 3)
	68.02	67.94	1.29	1.31	(1 1 2)

Table 1. Comparison of XRD peaks and interplanar distance values of fabricated ZnO thin films with standard JCPDS data sheet (00-036-1451).

Sample	Crystallite size (nm)
As prepared	6.1442
100°C	6.8793
120°C	6.9322
140°C	7.5700

Table 2. Variation of crystallite size D with annealing temperature of RF sputtered ZnO thin films.

3.1.2 Raman spectra analysis

Figure 1(b) represents the Raman spectra of ZnO thin films. The spectra featured attributes to the Raman active modes of ZnO hexagonal wurtzite crystal (K. Nakamoto, 1986). Hexagonal wurtzite type ZnO falls under the space group P_63mc . The optical Raman phonons of ZnO at the zone center is given by the irreducible representation $\Gamma=1A_1+1E_1+2E_2+2B_1$ where $1A_1$ and $1E_1$ represents Raman and infrared active modes and polar modes, which possess two branches namely longitudinal optical (LO) and transverse optical (TO) phonon associated with different wavelength. $2E_2$ is a non-polar Raman active mode consist of low-frequency mode (E_{2L}) associated

with vibration of Zn heavy ions and high-frequency mode (E_{2H}) associated with oxygen vibration. The $2B_1$ are two silent modes which are inactive in Raman spectra. (Bundesmann, C. 2003; Damen et al., 1966.) The Raman mode at 560.83cm^{-1} is assigned to $A_1(\text{LO})$ phonon mode, which is usually related to the oxygen vacancy and zinc interstitial. (das et al, 2011). The intensity of this Raman peak is noticed to be increasing which attributes to the excess zinc in the ZnO film (R. Mahendran,2013). The peak located at 1092.52cm^{-1} is attributed to 2LO phonons which is the characteristic of II-IV semiconductor. (D. N. Montenegro, 2013).

3.2 Optical properties

3.2.1 Transmission spectra analysis

Figure 2 depicts the transmission spectra of the as prepared and annealed ZnO thin films and absorbance spectra in the inset. Effect of annealing on the transmission property is manifested vividly. Results show that, as prepared ZnO thin films showed an improved transmission, while the transmission of annealed samples exhibited a slight reduction. In the inset of transmittance spectra, absorbance spectra are also plotted. Variations in value of absorbance is noticeable only near wavelength range lesser than 450nm. This indicate that the synthesized ZnO materials are suitable for photovoltaic applications, owing to a pronounced increase in absorbance within the strong absorption region corresponding to wavelengths below 450 nm (N. Ekema 2009).

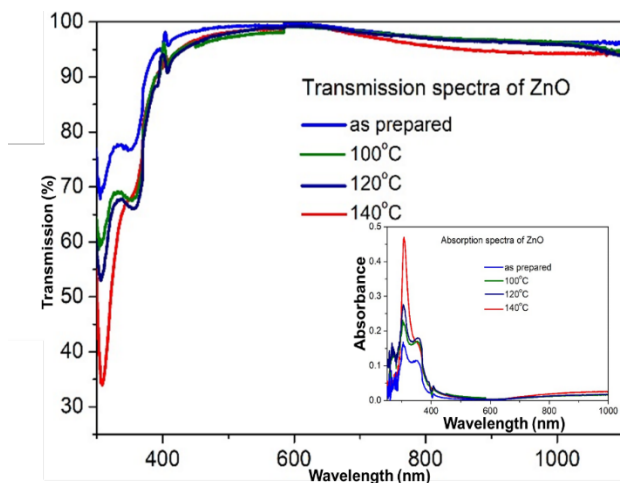


Figure 2. Transmission spectra of as prepared and annealed of RF sputtered ZnO thin films with absorbance spectra in the inset.

In the strong absorption region, the linear absorption coefficient, α , can be calculated from the following equation:

$$\alpha = 2.303 (A/t), \text{-----3, in terms of absorbance, A}$$

3.2.2 Energy Bandgap studies

The optical bandgap of a material denotes the minimum photon energy required to induce an electronic transition from the valence band to the conduction band via optical absorption. The primary distinction between the optical bandgap and the electrical bandgap of a material arises from the exciton binding energy, which represents the energy required to dissociate an electron-hole pair generated during photon absorption. Both the optical and electrical bandgaps are comparable for materials with extremely low exciton binding energies. Tauc plot was used to determine the optical bandgap where $(\alpha h\nu)^n$ vs $h\nu$ was plotted and it's given by the equation 4. Reports suggests that ZnO is a direct bandgap material (H. Afifi, 2010; F. Yakuphanoglus,2007) and therefore $n = 2$. This is clear from the Tauc plot also, as the linear portion of the curve is evidence of a direct optical transition in the material.

$$\alpha = A \frac{(h\nu - E_g)^n}{h} \text{-----4}$$

Optical bandgap was calculated from the intersection of the linear fit with x axis when $(\alpha h\nu)^n = 0$ (Chaabouni F, 2007). Figure 3 manifests the results obtained from Tauc plot of as prepared and annealed ZnO thin films. The band gaps of ZnO thin films were 3.49eV, 3.24eV, 3.22eV and 3.17eV corresponding to the as prepared and those annealed at 100°C ,120°C and 140°C respectively. The bandgap is found to be decreasing as the annealing temperature increased which is due to the change in the stoichiometry of the deposited films. In the case of a polycrystalline material which possess many grain boundaries, production of free carrier concentrations occurs at these sites. This increases the potentials at the grain boundaries creating an electric field which in

turn increases the energy gap of the material. Upon heating, the effect gets reduced due to the modification of the grain boundaries and hence the bandgap reduces (S. John, 2023).

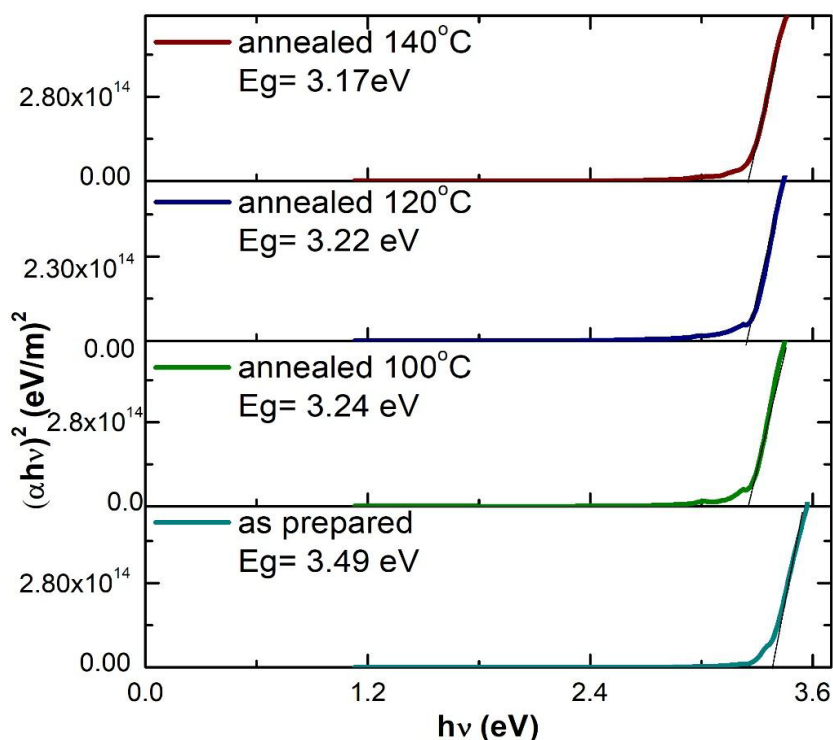


Figure 3. Energy bandgap plot of as prepared and annealed RF sputtered ZnO thin films

3.2.3 Refractive index, optical conductivity and extinction coefficient

Refractive Index

The electrical and optical properties of semiconductors show a profound dependence on refractive index (N. Baydogan 2013). Reports suggest that it is always better to have high refractive index, so that such materials could enhance the ability to trap more amount of light rays' incident on them (M. Ma,2011). Equation 5 was used to determine the refractive index where R is the reflectance. Figure 4(a) shows the dependency of refractive index on photon wavelength.

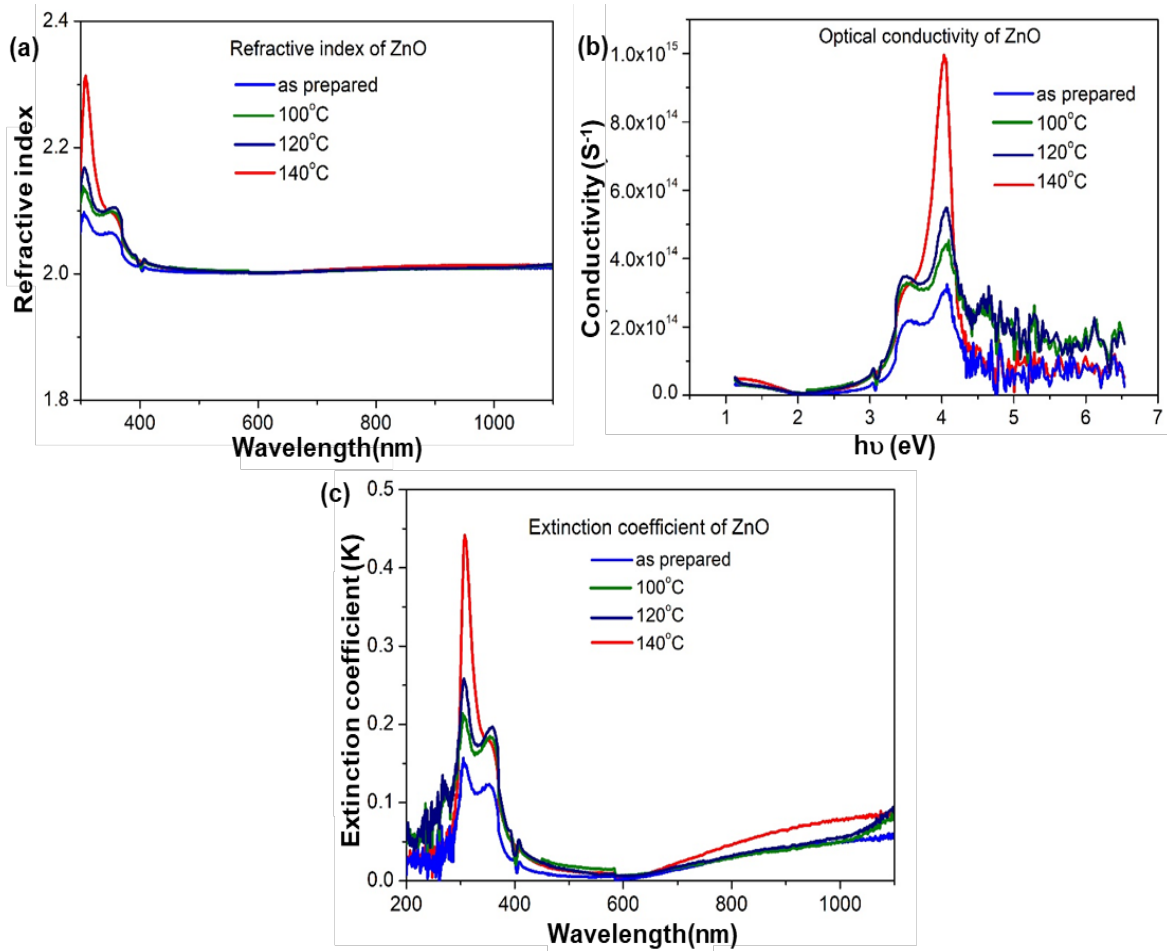


Figure 4(a) Refractive index spectra of as prepared and annealed RF sputtered ZnO thin films.
 (b) Optical conductivity spectra of as prepared and annealed RF sputtered ZnO thin films.
 (c) Variation of extinction coefficient with photon wavelength of as prepared and annealed RF sputtered ZnO thin films.

$$n = \frac{1 + \sqrt{R}}{1 - \sqrt{R}} \text{-----5}$$

The refraction index as a function of photon wavelength has been computed and displayed in Figure 4(a). At high wavelengths (> 400 nm), ZnO has a refractive index of 2, which is consistent with the reported values (S.H. Mohamed,2011).

Optical conductivity

The optical conductivity of the deposited material can be calculated using the following relation.

$$\text{conductivity} = \frac{\alpha n c}{4\pi} \text{-----} 6$$

α , n and c denote the absorption coefficient, refractive index and speed of light respectively.

Figure 4(b) depicts the dependency of optical conductivity spectra of as prepared and annealed ZnO thin films on photon energy.

Extinction coefficient

The ability of the material to absorb light at any given wavelength is denoted using extinction coefficient, k . The equation 7 relates extinction coefficient k , absorption coefficient α and wavelength λ , and is given below.

$$k = \frac{\alpha \lambda}{4} \text{-----} 7$$

Figure 4(c) shows the variation of extinction coefficient with photon wavelength of as prepared and annealed ZnO thin films. The values are in agreement with previous results (F. Yakuphanoglus, 2007).

6 Conclusion

ZnO thin films were successfully prepared by RF sputtering technique followed by annealing process. A comprehensive study on the effect of annealing process on the structural and optical properties of ZnO thin films was done. XRD analysis showed that the films obtained belongs to hexagonal wurtzite structure of ZnO. From XRD studies, absence of unknown peaks ensured that films are devoid of impurities and (100), (101) were the major planes of orientation of fabricated samples. Raman analysis was in agreement with the results obtained from XRD exhibiting two prominent peaks; one attributed to $A_1(\text{LO})$ phonon mode and other assigned to 2LO phonons of ZnO films. Optical properties such as transmittance, refractive index, extinction coefficient, optical conductivity and Tauc plot over a spectral range of 400–1000 nm have been

examined. A good optical transmittance has been observed for visible region, and the optical bandgap of as prepared ZnO films was found to be 3.49 eV and on annealing, the band gap showed a red shift by monotonously decreasing to 3.17eV. Band gap of annealed films showed a trend to decrease as the annealing temperature increases. The studies shows that post deposition annealing process is important step for improving the quality as well as crystallinity of ZnO thin films. Results from the current work strongly suggest that ZnO thin films fabricated, exhibited excellent properties which could opt as a good candidate for optoelectronic device applications.

Acknowledgements

The authors would like to acknowledge the Department of Science and Technology (DST- FIST), India for the financial support rendered in setting up the research lab (grant number SR/FST/College-237/2014 (C)). The services rendered by CIF, IIT Palakkad in the form of XRD and Raman analysis is also duly acknowledged.

References

1. Laurent K, Yu DP, Tusseau-Nenez S, Leprince-Wang Y. (2008). *Thermal annealing effect on optical properties of electrodeposited ZnO thin films*. Journal of Physics D: Applied Physics.
2. Arpana Agrawal, Tanveer Ahmad Dar, Pratima Sen (2013). *Structural and Optical Studies of Magnesium Doped Zinc Oxide Thin Films*. Journal of nano- and electronic physics
3. Jin ZC, Hamberg I, Granqvist CG. (1988). *Optical properties of sputter-deposited ZnO:Al thin films*. Thin Solid Films.
4. Ronen Gertman, Anna Osherov, Yuval Golan, Iris Visoly-Fisher. (2014). *Chemical bath deposited PbS thin films on ZnO nanowires for photovoltaic applications*. Thin solid films.

5. Oleg Lupan , Guangyu Chai , Lee Chow. (2008) *Novel hydrogen gas sensor based on single ZnO nanorod*. Microelectronic Engineering.
6. Ozgur U., Alivov, Y.I., Liu C., Teke A., Reshchikov M.A., Dogan S., Avrutin V., Cho S.J., A. (2005) *Comprehensive review of ZnO materials and devices*. Journal of Applied Physics.
7. M.N. Kamalasanan, S. Chandra. (1996). *Sol-gel synthesis of ZnO thin films*. Thin Solid Films.
8. F.D. Paraguay, W.L. Estrada, D.R.N. Acosta, E. Andrade, M. Miki-Yoshida. (1999) *Growth, structure and optical characterization of high quality ZnO thin films obtained by spray pyrolysis*. Thin Solid Films.
9. T. Minami, H. Sonohara, S. Takata, H. Sato. (1994). *Physical and Structural Properties of ZnO Sputtered Films*. Japanese Journal of Applied Physics.
10. K. Nakamura, T. Shoji, K. Hee-Bog. (2000). *Epitaxial Growth of 3C-SiC on an 8° -Off-Axis 6H-SiC (0001) Substrate*. Japanese Journal of Applied Physics.
11. S. Maniv, A. Zangvil. (1978). *Controlled texture of reactively rf-sputtered ZnO thin films*. Journal of Applied Physics.
12. Smiya John, K. Anlin Lazar, A. P. Reena Mary, V. Geetha. (2023). *Simulation and fabrication of ZnO/SiO₂-based 1D Photonic crystals for light trapping application*. Journal of optics.
13. Shashikant Sharma, Sumit Vyas, C. Periasamy, P. Chakrabarti. (2014). *Structural and optical characterization of ZnO thin films for optoelectronic device applications by RF sputtering technique*. Superlattices and Microstructures.
14. Cullity, B.D., S.R. Stock. (2001). *Elements of X-ray Diffraction*. Prentice hall New Jersey.
15. Patterson. (1939). *The Scherrer formula for X-ray particle size determination*. Physical review.
16. K. Nakamoto (1986). *Infrared and Raman Spectra of Inorganic and Coordination Compounds*. Fourth edition Wiley, New York.

17. Bundesmann, C., Ashkenov, N., Schubert, M., Spemann, D., Butz, T., Kaidashev, E.M., Lorenz, M., Grundmann, M. (2003). *Infrared Dielectric Functions and Phonon Modes of High-Quality ZnO Films*. Applied Physics Letters.
18. Damen, T.C., Porto, S.P.S., Tell, B. (1966). *Raman Effect in Zinc Oxide*. Physical Review.
19. Das J., Mishra D.K., Sahu D.R., Roul, B.K. (2011). *Influence of Ni doping on magnetic behavior of Mn doped ZnO*. Materials Letters.
20. R. Mahendran, Kashif, Saroja, Venkatachalam, Siva Kumar, Ayeshamariam, Sanjeeviraja, Hashim. (2013). *Structural and optical characterization of ZnO thin films annealed at different Temperatures*. Journal of Applied Sciences Research.
21. D. N. Montenegro, V. Hortelano, O. Martínez, M. C. Martínez-Tomas, V. Sallet, V. Muñoz-Sanjosé, J. Jiménez. (2013). *Non-radiative recombination centres in catalyst-free ZnO nanorods grown by atmospheric-metal organic chemical vapour deposition*. Journal of Physics D: Applied Physics.
22. N. Ekema, S. Korkmaza, S. Pata, M.Z. Balbagb, E.N. Cetina, M. Ozmumcua. (2009). *Some physical properties of ZnO thin films prepared by RF sputtering technique*. International journal of hydrogen energy.
23. H. Afifi, M. Abdel-Naby, S. El-Hefnawie, A. Eliewa, N. Ahmad. (2010). *Optical and Electrical Properties of Zinc Oxide thin film prepared by spray pyrolysis*. Iraqi Journal of Applied Physics.
24. F. Yakuphanoglus, S. Ilican, M. Caglarb, Y. Cagla. (2007). *The determination of the optical band and optical constants of noncrystalline and crystalline ZnO thin films deposited by spray pyrolysis*. Journal of Optoelectronics and Advanced Materials.
25. Chaabouni F, Abaab M, Rezig B. (2004). *Effect of the substrate temperature on the properties of ZnO films grown by RF magnetron sputtering*. Material Science and Engineering.
26. S. John, M. Francis, A. P. Reena Mary, V. Geetha. (2023). *Influence of annealing on the properties of chemically prepared SnS thin films*. Chalcogenide Letters.

27. N. Baydogan, T. Ozdurmusoglu, H. Cimenoglu, A.B. Tugrul. (2013). *Refractive index and extinction coefficient of ZnO:Al thin films derived by sol-gel dip coating technique*. Defect and Diffusion Forums.
28. M. Ma, F.W. Mont, X. Yan, J. Cho, F. Schubert, G.B. Kim, C. Sone. (2011). *Effects of the refractive index of the encapsulant on the light-extraction efficiency of light-emitting diodes*. Optics Express.
29. S.H. Mohamed. (2011). *Synthesis, structural and elliposmetric evaluation of oxygen-deficient and nearly stoichiometric zinc oxide and indium oxide nanowire/nanoparticles*. Philosophical Magazine.